Carpathian Journal of Earth and Environmental Sciences, August 2026, Vol. 21, No. 2, p. 321 – 332; DOI:10.26471/cjees/2026/021/371

GEOTHERMAL FIELD CHARACTERISTICS AND HEAT ACCUMULATION MECHANISMS OF THE YIMENG UPLIFT, ORDOS BASIN, CHINA

Lu LUO[1,2], Ruifeng KE[3,4*], Shaochuan SUN[1,2], Xiaoxue JIANG[3,4], Zihan Bao[3,4], Yanxin WANG[1,2], Xiang MAO[1,2], Chuanqing ZHU[3,4], Fang Xie[3,4] & Shudi XING[3,4]

[1]State Key Laboratory of Deep Geothermal Resources, Sinopec (Beijing) Research Institute of New Energy Technology Co., Ltd. Beijing 100083, China

[2]Sinopec Star Petroleum Co., Ltd., Beijing 100083, China

[3]State Key Laboratory of Deep Geothermal Resources, China University of Petroleum (Beijing), Beijing, 102249, China

[4]College of Geosciences, China University of Petroleum (Beijing), Beijing, 102249, China

**Corresponding author: 2416281599@qq.com*

Abstract: The Yimeng Uplift is located at the northern margin of the Ordos Basin, China, and represents an important structural unit with potential for medium- and low-temperature geothermal resources. Based on drilling temperature data, together with rock thermal conductivity, radiogenic heat production, and groundwater hydrochemical data, this study investigates the characteristics and possible controlling factors of the present-day geothermal field in the study area. The results show that the average geothermal gradient in the Yimeng Uplift is 28.9 °C/km and the average terrestrial heat flow is 66.2 mW/m^2, indicating a moderate to moderately high thermal background within the Ordos Basin. The geothermal field is interpreted to be mainly conduction-dominated and to exhibit a “hot crust–cold mantle” thermal structure, with no clear evidence of anomalous deep-seated thermal enhancement. The geothermal field also shows a clear shallow–deep differentiation. The shallow thermal field appears to be influenced by basement relief, variations in sedimentary cover structure, thermophysical heterogeneity, and local hydrogeological conditions, whereas the deep thermal field more closely reflects the regional deep thermal background under steady-state conductive conditions. Overall, the geothermal regime of the Yimeng Uplift can be summarized as a conceptual model of regional deep thermal background with shallow stratigraphic and hydrogeological modulation. These results provide a geological basis for the evaluation and development of medium- and low-temperature geothermal resources in the Yimeng Uplift.

Keywords: Yimeng Uplift, geothermal gradient, heat flow, controlling factors, geothermal field

1. INTRODUCTION

Driven by global energy scarcity and China’s "Dual Carbon" goals (carbon peaking and carbon neutrality), geothermal energy – a clean, renewable, and baseload energy resource – is assuming an increasingly pivotal role (Lin et al., 2013; Wang et al., 2020; Wang et al., 2017; Gu et al., 2007). In comparison with intermittent renewable energy sources (e.g., solar and wind energy), geothermal energy offers distinct advantages: abundant resource reserves, high energy conversion efficiency, and stable baseload operation. These merits endow it with broad prospects for development and application. As a major energy basin in China, the Ordos Basin is rich in low-to-medium temperature hydrothermal geothermal resources both within and around its boundaries (Wang et al., 2004). The Yimeng Uplift, located on the northern margin of the basin, is a key tectonic unit characterized by significantly higher heat flow compared to the rest of the basin. This unique thermal feature further highlights its great potential for geothermal resource development (Li, 2021; Huang et al., 2015; Ding, 2010; Sun et al., 1996; Ren et al., 2020; Zhao, 2016; Ren & Zhao, 1997; Ren, 2000).

Research on the geothermal field of the Ordos Basin originated in the 1990s, initially driven by

mineral and hydrocarbon exploration campaigns. Early studies primarily focused on the basin's thermal evolution, revealing that the paleogeothermal gradient during the Late Mesozoic was significantly higher than present-day levels. Spatially, the contemporary geothermal field exhibits a "high-east, low-west" distribution pattern, with an average heat flow of 64.7 ± 8.9 mW/m^2 (Li et al., 1996), and prominent thermal anomalies have been identified along the basin margins (Ren, 1998). With the advancement of regional investigations, the Yimeng Uplift has emerged as a focal point due to its distinct geothermal signature. It is characterized by a geothermal gradient of 27-31 °C/km, aligning with medium-temperature geothermal systems (Ren, 1998; Ren et al., 2006). Recent tectonic and numerical analyses suggest that these anomalies are fundamentally controlled by basement uplifts and faulting activities (Wang et al., 2004). Notably, the heat flow in the Yimeng Uplift exceeds the basin average, reflecting a "hot crust and cold mantle" lithospheric thermal structure (Huang et al., 2015), which provides a unique deep-seated background for geothermal resource accumulation.

Despite these advances, the geothermal regime of the Yimeng Uplift remains poorly understood due to scarce geological data, uncertain controlling factors, and the lack of a clear genetic model. These knowledge gaps impede the effective exploration and development of the region's geothermal resources. To address these gaps, this study integrates temperature data from over 70 wells, thermophysical properties of 110 rock samples, and hydrochemical data. Specifically, we aim to: (1) accurately characterize the spatial distribution characteristics of the contemporary geothermal field in the Yimeng Uplift; (2) comprehensively analyze the controlling factors from multiple perspectives, including deep-seated tectonic settings and shallow-buried rock thermophysical properties; and (3) establish a genetic model of geothermal resources in the study area. This work aims to provide a scientific basis for the efficient exploration and sustainable development of geothermal resources in the Yimeng Uplift.

2. GEOLOGICAL SETTING

The Ordos Basin, situated in the western North China Craton (NCC), is divided into six tectonic units: the Yishan Slope, the Jinxi Fold Belt, the Tianhuan Depression, the Western Margin Thrust Belt, the Weibei Uplift, and the Yimeng Uplift (Deng et al., 2005). As a prominent tectonic element, the Yimeng Uplift is delimited to the north by the Southern Margin Fault of the Hetao Graben, to the west by the Eastern Piedmont Fault of the Zhuozishan Mountains, and to the east by the Lishi Fault. Its southern boundary is defined by a southward-protruding, arc-shaped gravity and magnetic anomaly zone (Wang, 2011) (Figure 1). The stratigraphic succession in the study area, in ascending order, comprises Archean, Proterozoic, Paleozoic, and Mesozoic strata, capped by relatively thin Cenozoic sediments (Tian, 2023; Zhang, 2017; Quan, 2020; Qiao, 2013; Wei, 2023). Lithologically, the Archean basement consists mainly of metamorphic and granitic rocks, whereas the Proterozoic succession includes clastic and carbonate rocks with locally developed granitic and gneissic basement components. The Paleozoic strata are dominated by marine carbonate and clastic rocks, the Mesozoic succession mainly consists of continental clastic deposits, and the Cenozoic cover is relatively thin and composed chiefly of unconsolidated sediments. Because Figure 1 is a regional-scale surface geological map, localized exposures of Archean and Proterozoic basement rocks are not fully represented due to map scale and limited surface exposure.

3. THERMAL PHYSICAL PROPERTIES

3.1. Thermal conductivity of rocks

Thermal conductivity was determined for 82 outcrop samples collected from three representative sampling regions (BT, WH, and WZ, as indicated in Figure 1). Measurements were conducted using a HotDisk thermal constant analyzer based on the transient plane source (TPS) method, with a relative uncertainty within ±3% (Tang et al., 2021).

The test results (Figure 2) indicate that the thermal conductivity of outcrop samples from the Yimeng Uplift ranges from 1.22 W/(m·K) to 5.85 W/(m·K), with an average value of 3.27 ± 0.92 W/(m·K). Across the sampled lithologies, metamorphic rocks exhibit the highest average thermal conductivity (2.97 ± 0.95 W/(m·K)), followed by igneous rocks (2.88 ± 0.41 W/(m·K)), while sedimentary rocks have the lowest average thermal conductivity (2.53 ± 0.88 W/(m·K)). Significant variations in thermal conductivity are also observed among different sedimentary lithologies: limestone has the highest thermal conductivity (3.74 W/(m·K)), followed by quartz sandstone (3.24 W/(m·K)), and mudstone has the lowest (1.77 W/(m·K)). These results demonstrate that lithology-controlled differences in thermal conductivity directly affect the thermal transfer characteristics of rock masses in the study area and are closely associated with the formation and distribution of the geothermal field.

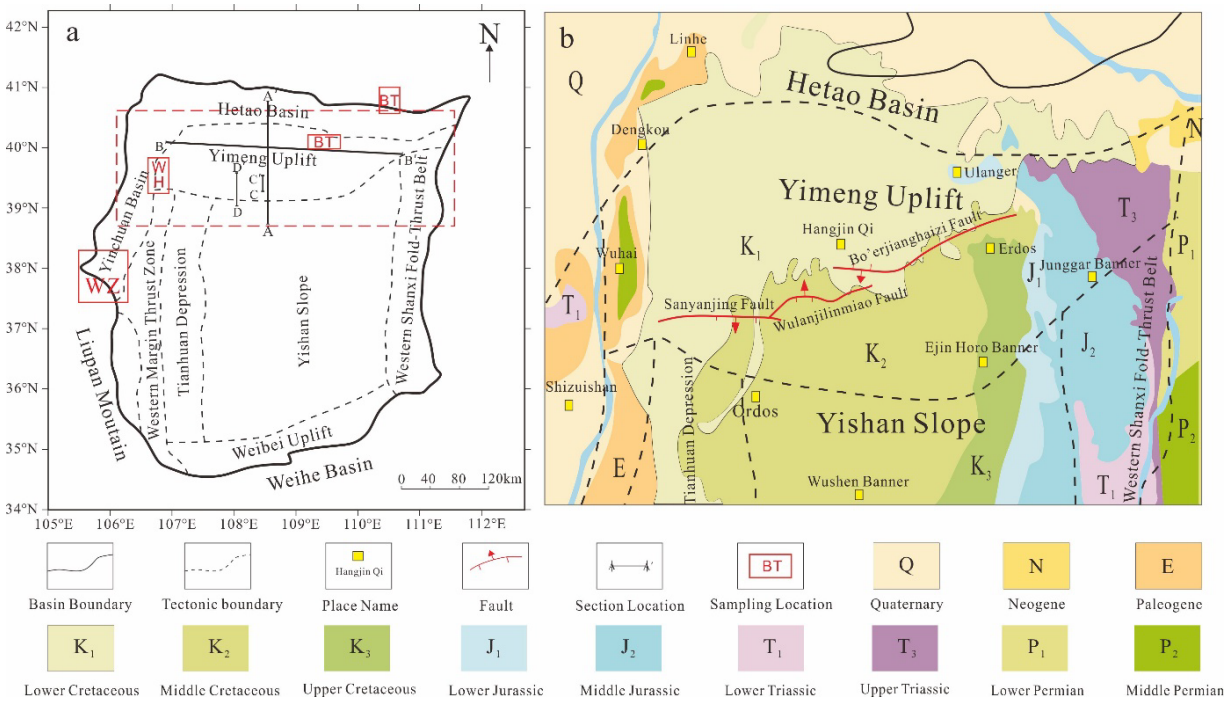

Figure 1. Structural setting and stratigraphic distribution of the Yimeng Uplift and adjacent areas in the Ordos Basin (Wang et al., 2016; Wang et al., 2019; Sun et al., 2017); a) location map of the Ordos Basin and the Yimeng Uplift; b) Geological map of the Yimeng Uplift and surrounding areas.

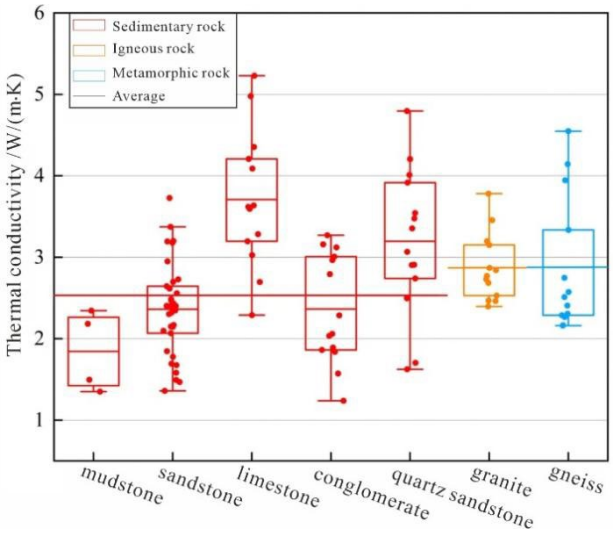

Figure 2. Statistical distribution of rock thermal conductivity.

Given the hydrothermal characteristics of the system, saturation corrections were applied to the sandstone reservoir data for subsequent heat flow and temperature calculations. For deep-seated carbonate, igneous, and metamorphic rocks, temperature-dependent empirical formulas were employed (Yu et al., 2017).

3.2. Radiogenic heat production rate of rock

The radiogenic heat production (A) generated by the decay of radioactive elements (U, Th, and K) constitutes a primary internal heat source for the crust. As a critical parameter alongside thermal conductivity, the radiogenic heat production rates in the Yimeng Uplift were systematically compiled from previous studies (Yu et al., 2017; Ren et al., 2007; Zhang, 1994; Zhang, 2006) and supplemented with new measurements. These values were calculated using the Rybach empirical formula (Shao et al., 2025). Consequently, a regional distribution map (Figure 3) and a statistical summary (Table 1) of the heat production rates were established. These datasets, integrated with the corrected thermal conductivity values, provide a robust multi-dimensional framework for subsequent geothermal anomaly analysis and reservoir temperature modeling.

$$A = 0.01\rho(9.52CU + 2.56CTh + 3.48CK) \quad (1)$$

where, A represents the radioactive radiogenic heat production (rate) of the rock sample, with the unit of μW/m³; ρ represents the density of the rock sample, with the unit of g/cm³; *CU* and *CTh* represent the contents of radioactive elements U and Th in the rock, respectively, with the unit of ppm; and *CK* represents the mass fraction of K in the rock, with the unit of %.

Results from a total of 75 radiogenic heat production (RHP) data points indicate that the shallow strata in the study area are characterized by relatively high RHP rates, with distinct inter-lithological variations. Mudstone exhibits the highest

average RHP of approximately 2.10 μW/m³, identifying it as the primary shallow heat-contributing lithology. In contrast, sandstone and carbonate rocks yield lower averages of 1.31 μW/m³ and less than 1.0 μW/m³, respectively. These lithology-specific heat production capacities provide a non-negligible contribution to the shallow crustal heat flow.

By integrating thermal conductivities with these RHP distributions, a comprehensive thermal property profile was established as summarized in Table 1. To ensure physical consistency, the representative stratigraphic values in Table 1 were determined based on lithological proportions. Specifically, the stratigraphic thermal conductivity (K) was derived using the harmonic average, while the stratigraphic RHP (A) was calculated using a weighted arithmetic average. This dual-averaging approach provides a robust basis for the subsequent geothermal anomaly analysis and reservoir temperature modeling.

4. DISTRIBUTION CHARACTERISTICS OF THE GEOTHERMAL FIELD

4.1. Distribution characteristics of the geothermal gradient

Based on static temperature data from the Yimeng Uplift and surrounding areas, the temperature-depth (T-D) relationships of the surveyed wells were analyzed systematically (Li, 2021; Ren et al., 2006; Qi, 2018). Overall, formation temperature shows a clear linear increase with burial depth (Figure 4), indicating that the present-day thermal field is mainly controlled by steady-state conduction. Nevertheless, several wells display localized thermal anomalies. Wells Meng 5 (41.4 ℃/km) and Yu 10 (42.7 ℃/km) have higher temperatures and steeper gradients than the regional trend, probably due to upward groundwater flow or shallow aquitards that restrict heat loss. By contrast, Wells E3 (17.7 ℃/km) and ER01 (22.1 ℃/km) show lower temperatures and gentler gradients, which likely reflect cooling caused by shallow groundwater recharge. These results suggest that, although conduction dominates at the regional scale, localized hydrogeological effects may contribute to local deviations from conductive heat transfer.

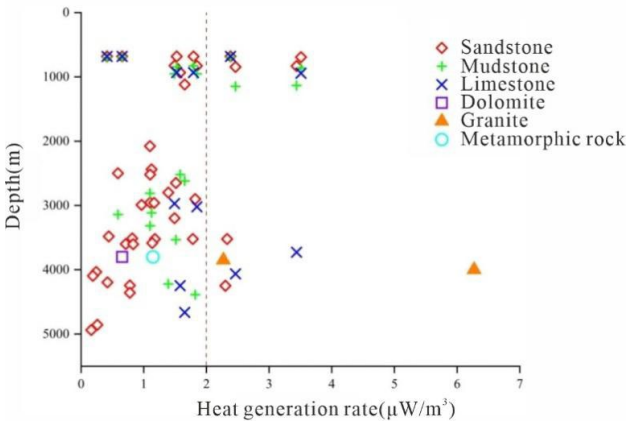

Figure 3. Distribution Map of Radiogenic Heat Production in Rocks in the Yimeng Uplift.

Table 1. Thermal Properties of Rocks in the Yimeng Uplift.

Stratum	Rock Composition					Harmonic Average Thermal Conductivity (W/(m·K))	Radiogenic heat production rate (μW/m³)
	Shale	Sandstone	Limestone	Granite	Gneiss		
Cenozoic Era（Q-E）	45%	55%				1.74±0.30 (n=11)	1.79±0.32 (n=12)
Cretaceous System（K）	20%	60%				2.37±0.60 (n=5)	1.60±0.67 (n=8)
Jurassic System（J）	10%	80%				3.03±0.58 (n=15)	1.30±0.28 (n=15)
Triassic System (T)	20%	80%				2.41±0.69 (n=5)	1.13±0.12 (n=5)
Late Paleozoic Erathem（C+P）	10%	70%	10%			3.01±0.43 (n=19)	1.58±0.81 (n=11)
Early Paleozoic Erathem（O+Є）		15%	85%			3.97±0.55 (n=18)	1.07±0.68 (n=16)
Proterozoic Eonothem（Pt）		10%	10%	60%	20%	2.54±0.37 (n=5)	1.05±0.83 (n=4)
Archean Eonothem（Ar）				30%	70%	2.49±0.36 (n=4)	1.13±2.01 (n=4))

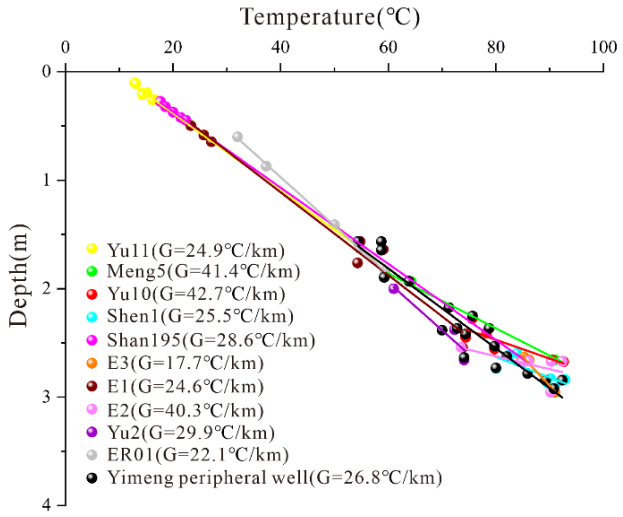

Figure 4. Present-day geothermal temperature versus depth relationship in the study area.

Extending from vertical profiles to spatial patterns, we investigated the regional variability of geothermal gradients. Utilizing Kriging interpolation on the integrated gradient datasets (Zhang, 2006; Shao et al., 2025; Qi, 2018; Wang & Huang, 1988), a spatial distribution map was generated (Figure 5). The map reveals that elevated geothermal gradients are primarily concentrated in the northern sector of the Yimeng Uplift and its adjacent areas, whereas the interior and southern margins exhibit relatively lower values. This pronounced north-south zonation underscores the spatial heterogeneity of the regional thermal regime, which is modulated by a synergistic complex of deep-seated tectonic and shallow hydrological factors.

4.2. Distribution characteristics of terrestrial heat flow

Integrating compiled heat flow datasets of China (Wang & Huang, 1988; Wang & Huang, 1990; Hu et al., 2001; Jiang et al., 2016), together with the updated geothermal gradients and harmonic mean thermal conductivities obtained in this study, we refined the heat flow database for the study area. The results show that heat flow in the Yimeng Uplift ranges from 59.7 to 73.1 mW/m^2, with a mean value of 66.2 mW/m^2. This value is slightly higher than both the continental average for China (63.0 ± 24.2 mW/m^2) (Jiang et al., 2016) and the overall mean for the Ordos Basin (64.7 mW/m^2), indicating a relatively favorable thermal background in the uplift. As shown in Figure 6, the spatial pattern of heat flow is not fully consistent with that of geothermal gradients. Rather than exhibiting a basin-scale trend, the study area shows several localized heat flow anomalies, mainly concentrated in the Wujiabao, Gongkahang, and Dongsheng depressions in the southern part of the uplift. These anomalies may be related to a combination of factors, including basement relief, variations in sediment thickness, thermal conductivity contrasts, and possible structurally enhanced permeability along major faults.

However, this interpretation is based mainly on spatial patterns and indirect evidence, and the relative contribution of these factors cannot be quantified with the currently available data. Outside these anomalous zones, heat flow remains within a generally moderate to moderately high range. Overall, the terrestrial heat flow pattern of the Yimeng Uplift can be characterized

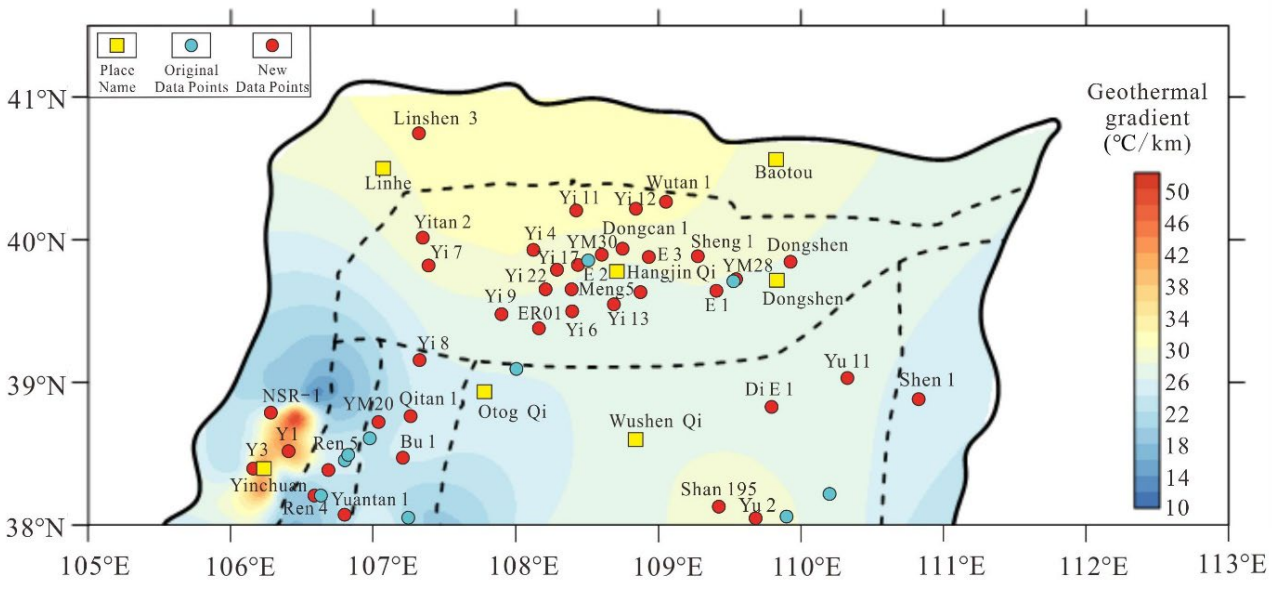

Figure 5. Geothermal gradient contour map of the Yimeng Uplift and adjacent areas.

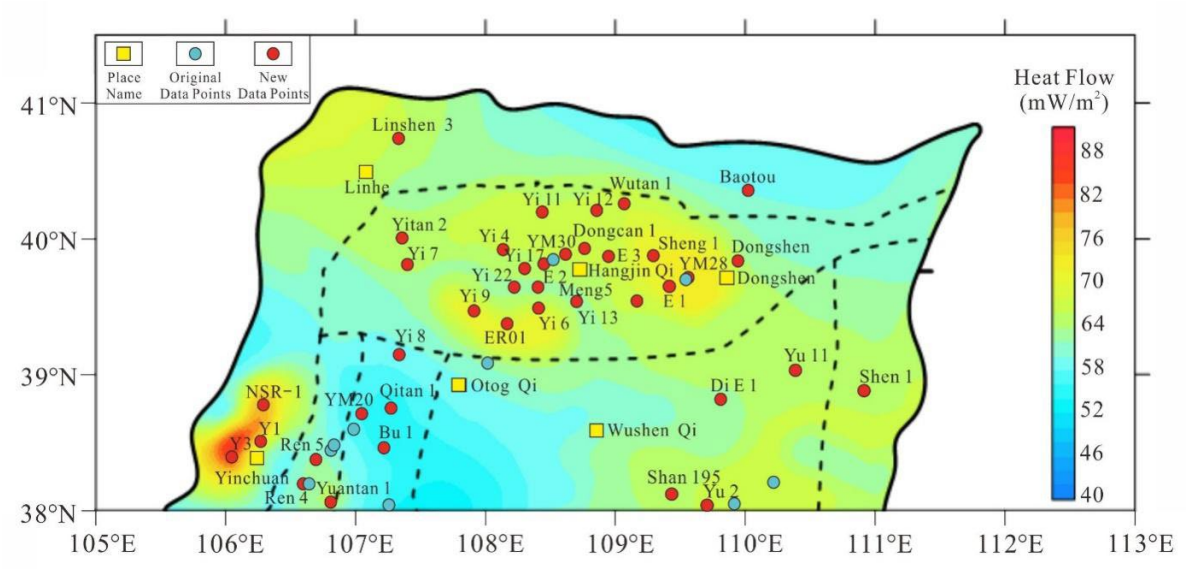

Figure 6. Terrestrial Heat Flow Contour Map of the Yimeng Uplift and adjacent areas.

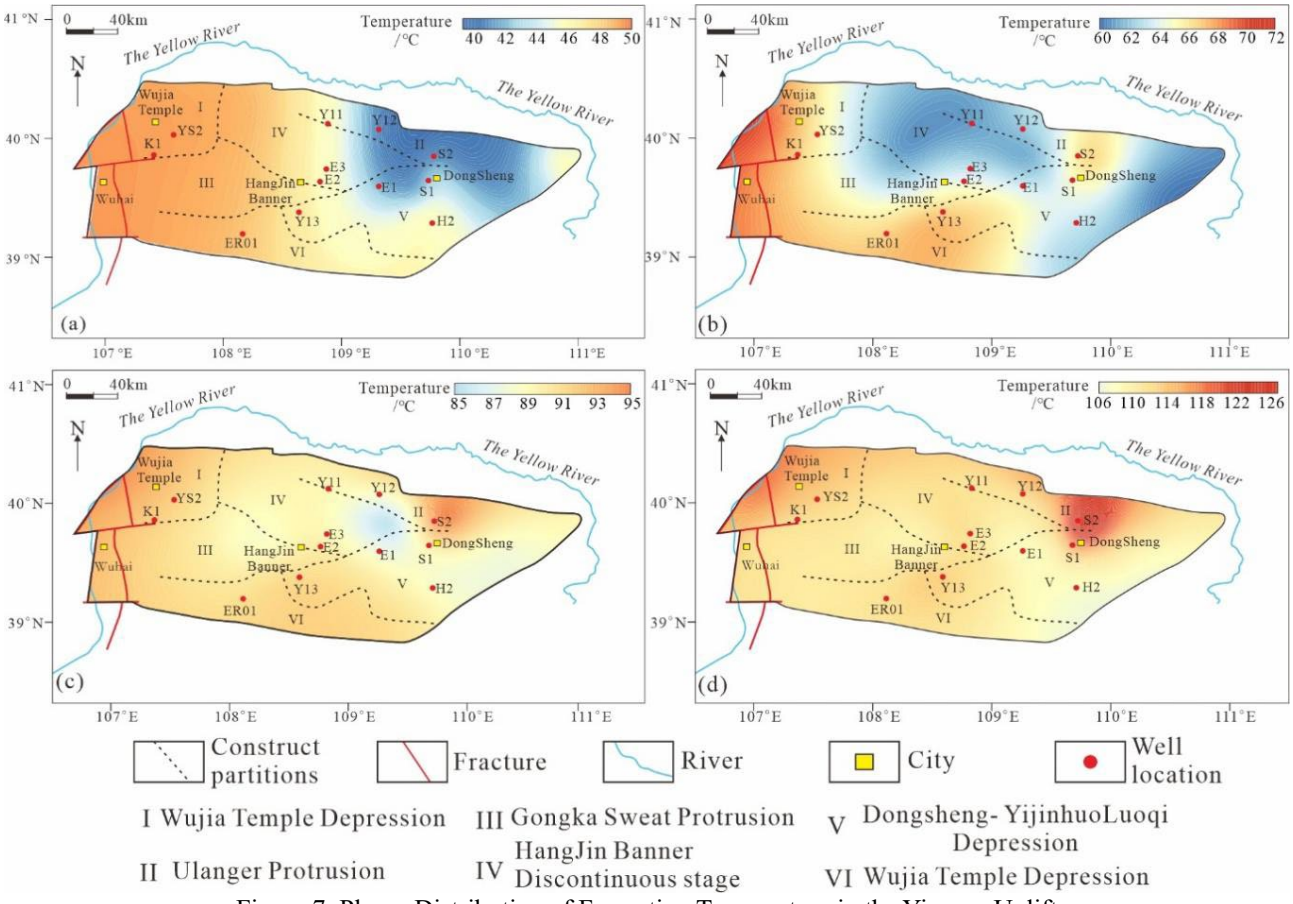

Figure 7. Planar Distribution of Formation Temperature in the Yimeng Uplift
(a)Temperature at 1000m (b)Temperature at 2000m (c)Temperature at 3000m (d)Temperature at 4000m.

as a relatively stable regional thermal background with superimposed localized anomalies, rather than a simple uniform trend.

4.3. Formation temperature

Due to the scarcity of deep borehole temperature logs, formation temperatures at depths of 1000 - 4000 m were estimated using a 1D steady-state conductive heat transfer model. This model was constrained by regional heat flow, lithology-specific thermal conductivity, and radiogenic heat production rates. Our results indicate that while temperatures generally increase with burial depth,

they exhibit significant spatial heterogeneity (Figure 7). At shallow depths (1000 - 2000 m), thermal anomalies are predominantly concentrated along the western and southern margins, showing a "south-high, north-low" and "west-high, east-low" distribution. Notably, with increasing depth (3000 - 4000 m), these high-temperature zones shift eastward, forming a prominent thermal belt across the Dongsheng-Yijinhuoluoqi region. This depth-dependent shift represents a transition from a west-dominated thermal regime to an eastward-shifted zonation. Collectively, the 3D temperature architecture reveals that the regional thermal field is not only depth-controlled but also modulated by a synergistic interplay between deep-seated tectonic-thermal settings and variations in the shallow conductive framework.

5. MAIN CONTROLLING FACTORS AND GENETIC MECHANISMS OF THE GEOTHERMAL FIELD

Synthesizing geothermal gradients, heat flow datasets, and depth-dependent temperature fields, we conclude that the contemporary thermal regime of the Yimeng Uplift is not a monolithic anomaly. Instead, it is characterized by localized high-temperature anomalies superimposed onto a moderate regional background, exhibiting significant vertical variations across stratigraphic intervals. Notably, heat flow and geothermal gradients are not linearly correlated. In specific areas, such as the Wujiamiao-Gongkahan region, high heat flow coincides with average geothermal gradients, indicating a complex coupling of multiple controlling factors. Overall, the thermal architecture of the Yimeng Uplift results from the synergistic interplay between deep crustal-mantle heat input, the thermal conductivity framework of the sedimentary cover, and localized fluid activity. While the deep-seated thermal structure exerts a primary regulatory role, the shallow caprock and fault systems modulate the heat transfer process, and localized fluid circulation further decorrelates the relationship between heat flow and formation temperatures.

5.1. Deep control factors

The Moho depth across the Ordos Basin ranges from 39 to 46 km with gentle undulations, indicating a relatively stable and moderately thick crust. In the Yimeng Uplift, the Moho depth varies between 37 and 43 km (Figure 8), and although localized shallowing is observed, the overall variation is limited, with no clear evidence of significant crustal thinning or strong deep-seated structural disturbance. This suggests that the deep structural setting of the study area remains broadly consistent with a stable cratonic framework.

To further assess the relative contributions of crustal and mantle heat flow, a simplified heat flow partitioning analysis was carried out for the Yimeng Uplift, as shown in Figure 9, by referring to previously published crustal layering models and thermophysical parameter settings for the Ordos Basin (Cai et al., 2007; Teng et al., 2010; Sun et al., 2013; Cheng et al., 2014). In this analysis, the crustal layering framework and the radiogenic heat production values of the upper, middle, and lower crust were adopted from previous studies, whereas the radiogenic heat production of the sedimentary cover and the regional average surface heat flow (66.2 mW/m^2) were constrained by the data compiled in this study. Based on this integrated approach, the qc/qm ratio (ratio of crustal to mantle heat flow) is estimated to be approximately 1.6. This value should be regarded as a regional average estimate rather than a site-specific result. It indicates that crustal radiogenic heat makes an important contribution to the total surface heat flow, which is consistent with a “hot crust - cold mantle” thermal structure. Therefore, the surface heat flow in the study area is interpreted to reflect the combined influence of crustal heat production and a relatively stable mantle heat flow background.

5.2. Shallow influencing factors

The spatial association between basement relief and high-heat-flow zones suggests that basement morphology may significantly influence upward heat conduction by modifying sedimentary cover thickness and effective thermal resistance (Figure 10). A comparative analysis of geothermal gradients (Figure 5) and heat flow distribution (Figure 6) reveals substantial spatial discrepancies. In particular, the Early Paleozoic uplift in the Yimeng region experienced intensified northward erosion, resulting in extensive truncation of Cambrian and Ordovician strata. This stratigraphic discontinuity likely modified the regional thermal conductivity framework. Specifically, thinning of the sedimentary cover may shorten the conductive path to the surface, while lithological contrasts within the truncated succession may alter the vertical distribution of thermal resistance. The combined effects of basement uplift and sedimentary cover thinning may therefore have redistributed heat conduction pathways and contributed to spatial variations in geothermal gradients under a similar regional heat-flow background.

Although fault structures are well developed in the study area, the available heat flow data do not

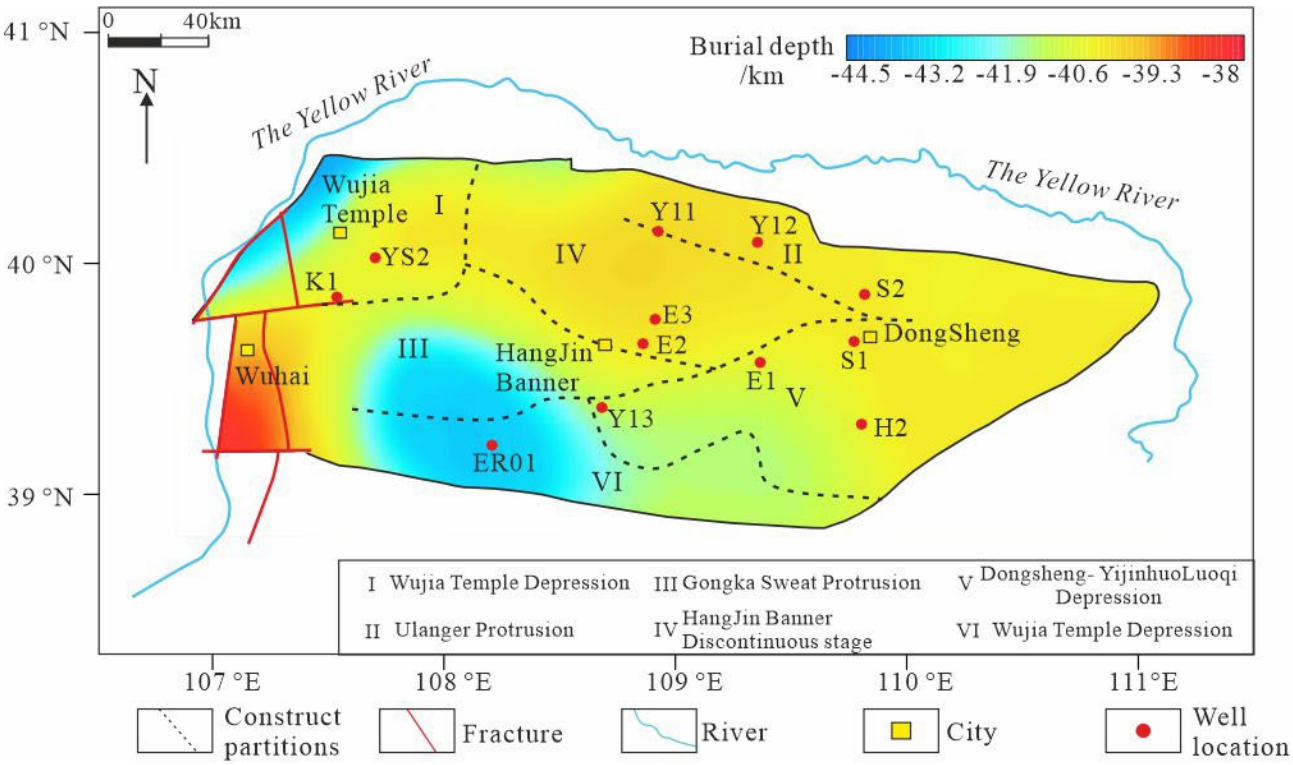

Figure 8. Distribution of burial depth of Moho discontinuity in Yimeng uplift.

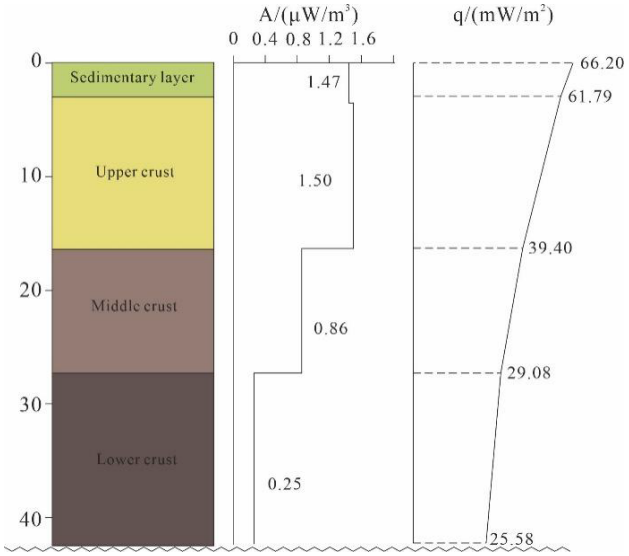

Figure 9. Simplified heat flow partitioning model of the Yimeng Uplift based on a layered stripping approach.

show a clear spatial correspondence between regional heat flow anomalies and mapped fault traces. This suggests that, under the relatively stable cratonic setting of the Yimeng Uplift, faults are unlikely to act as the primary control on the regional thermal background. However, they may still locally influence shallow heat transfer and groundwater circulation through permeability enhancement. In addition, deviations from linear shallow temperature-depth relationships may reflect localized hydrogeological effects, which could contribute to departures from the regional steady-state conductive pattern.

Hydrochemical characteristics of groundwater provide supplementary evidence for fluid regime differences in the study area (Sun et al., 2024; Zhao et al., 2022; Guo et al., 2009). Shallow groundwater is predominantly of the HCO3-Ca type with relatively low Total Dissolved Solids (TDS), which generally reflects open hydrogeochemical conditions and relatively frequent water-rock interaction. In contrast, deep formation water evolves toward the Cl-Na type with markedly higher TDS, suggesting more confined aquifer conditions and relatively limited fluid exchange (Figure 11). These hydrochemical differences indicate a clear vertical differentiation between shallow and deep groundwater systems. Although the available hydrochemical data do not directly quantify fluid-flow intensity or its thermal effect, they are broadly consistent with the interpretation that shallow hydrogeological conditions may contribute to the spatial variability of the shallow geothermal field.

Thermal distribution results at different depths are also consistent with this interpretation. The shallow geothermal field (1000 - 2000 m) corresponds relatively well with geothermal gradients and heat flow patterns, whereas at greater depths (3000 - 4000 m), the thermal center shifts toward the eastern segment and becomes decoupled from the shallow high-temperature zones. This depth-dependent divergence suggests that the influence of shallow hydrogeological conditions and near-surface heterogeneity decreases with depth.

Accordingly, the deep thermal field is interpreted to be more strongly controlled by steady-state conduction and the broader deep-seated thermal architecture.

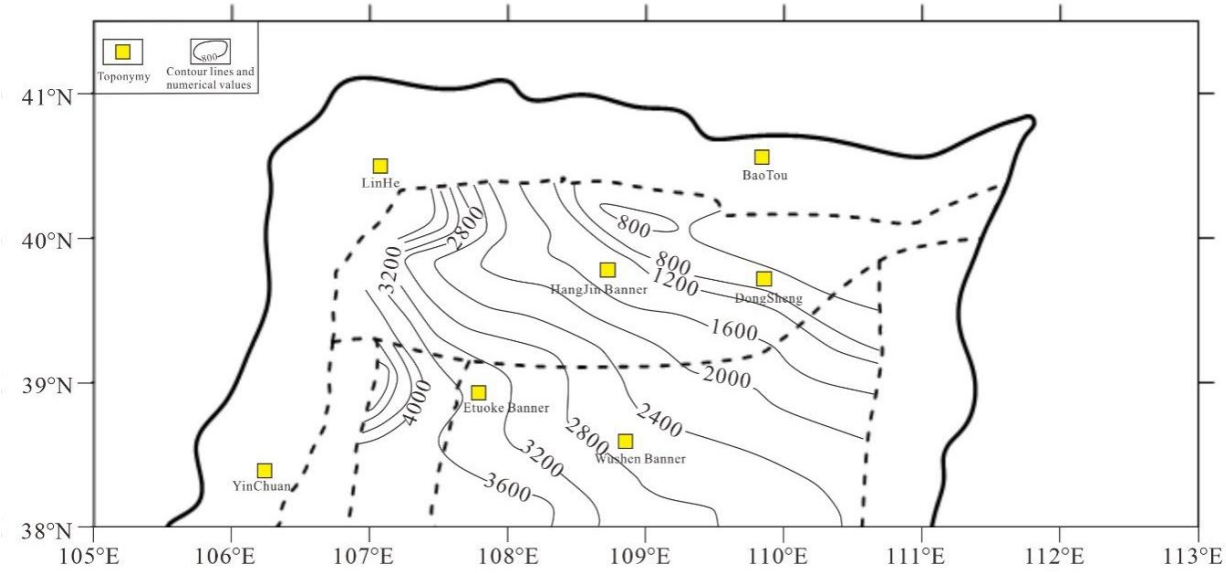

Figure 10. Depth to basement map of the study area (Yu et al., 2017).

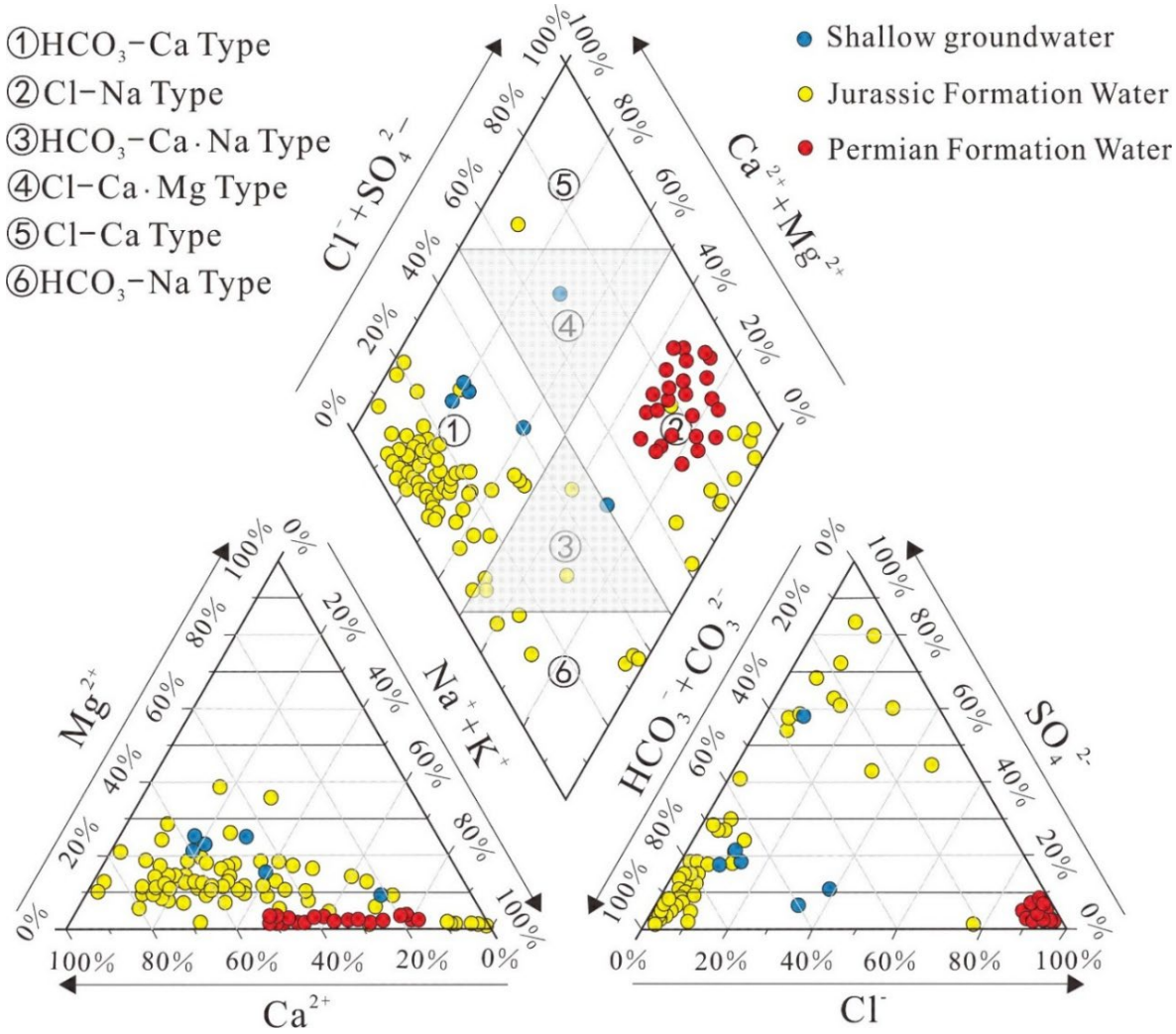

Figure 11. Piper diagram of groundwater chemical composition in the Yimeng Uplift (Sun et al., 2024; Zhao et al., 2022; Guo et al., 2009).

5.3. Genetic model of geothermal systems

Based on an integrated analysis of geothermal gradients, terrestrial heat flow, multi-depth temperature fields, and hydrochemical evidence, the geothermal regime of the Yimeng Uplift is interpreted to be developed on a relatively stable cratonic framework. Mantle heat flow appears to remain at a regional background level, with no clear evidence of anomalous deep-seated thermal enhancement.

Superimposed on this background, spatial variations in the shallow thermal field may be associated with a combination of factors, including basement relief, variations in sedimentary cover thickness, and thermophysical heterogeneity. Although fault structures are present in the study area, the available data do not show a clear correspondence between regional heat flow anomalies and mapped fault distributions. Therefore, faulting is not considered a primary control on the regional thermal regime, but may locally influence shallow heat transfer through limited permeability enhancement.

In addition, hydrochemical characteristics indicate a clear differentiation between shallow and deep groundwater systems, suggesting that shallow hydrogeological conditions may contribute to the spatial variability of the shallow geothermal field. However, there is no direct evidence to demonstrate that fluid circulation significantly perturbs heat transfer at depth.

With increasing depth, the influence of shallow heterogeneity and hydrogeological conditions appears to decrease, and the thermal field becomes increasingly dominated by steady-state conduction, which reflects the broader regional thermal structure.

At the current stage, this interpretation should be regarded as a qualitative conceptual framework based on the available geological, thermal, and hydrochemical evidence. More detailed structural constraints and quantitative analyses will be needed in future work to further evaluate the relative contributions of fracture networks and other controlling factors.

Accordingly, the geothermal field of the Yimeng Uplift can be described by a conceptual model of “regional deep thermal background with shallow stratigraphic and hydrogeological modulation” (Figure 12).

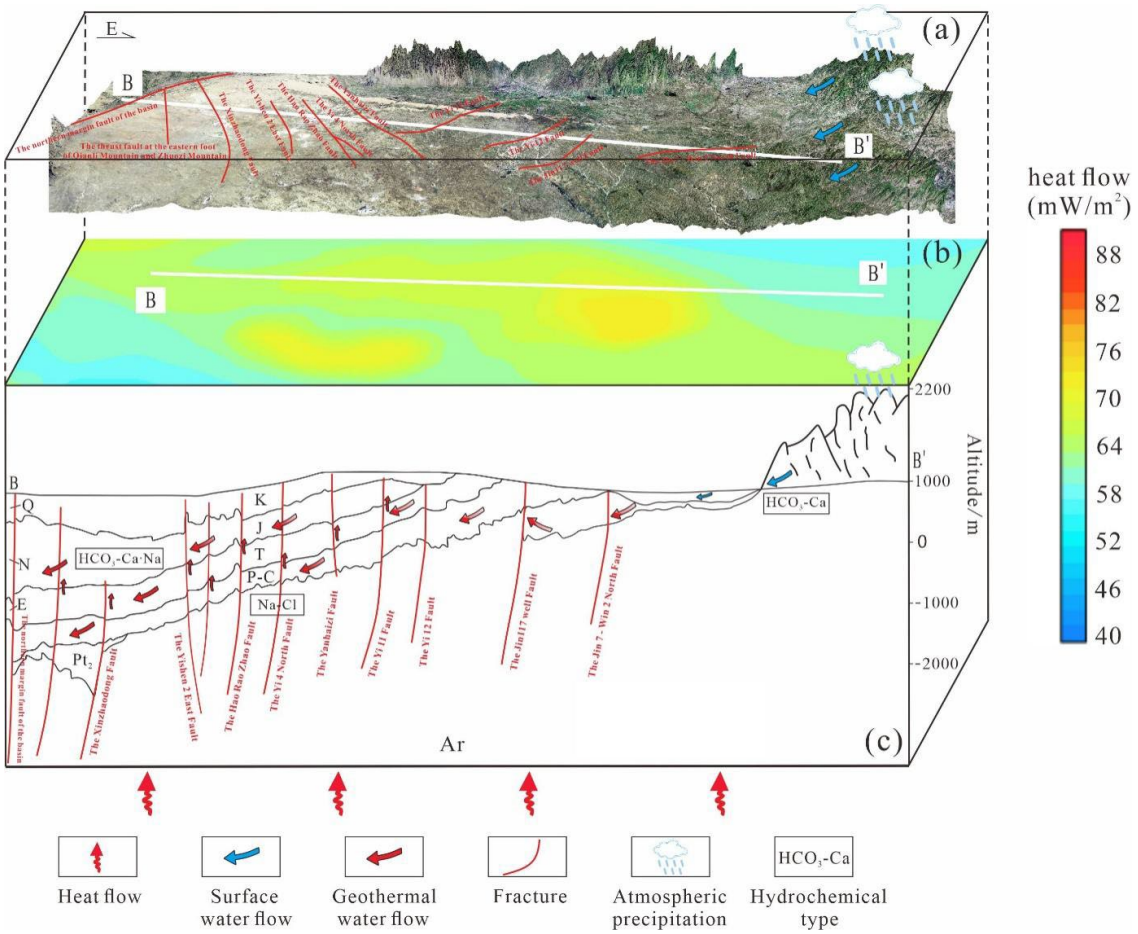

Figure 12. Conceptual model of geothermal field formation in the Yimeng Uplift; a) Topographic elevation map and major fault distribution; b) Surface heat flow distribution along the B–B′ profile; c) Geological cross-section illustrating the conceptual controls on the geothermal field.

6. CONCLUSIONS

(1) The average geothermal gradient in the Yimeng uplift area is 28.9 °C/km, and the average terrestrial heat flow is 66.2 mW/m^2, indicating a moderately high thermal background relative to the Ordos Basin.

(2) The geothermal field of the Yimeng Uplift is interpreted to exhibit a "hot crust–cold mantle" thermal structure, with no clear evidence of anomalous deep-seated thermal enhancement. The surface heat flow likely reflects the combined influence of crustal radiogenic heat production and regional background mantle heat flow.

(3) The geothermal field of the Yimeng Uplift shows clear shallow–deep differentiation. The shallow thermal field appears to be influenced by basement relief, variations in sedimentary cover, thermophysical heterogeneity, and local hydrogeological conditions, whereas the deep thermal field is more consistent with steady-state conductive control and the regional thermal background. Overall, the geothermal regime of the study area can be summarized as a conceptual model of "regional deep thermal background with shallow stratigraphic and hydrogeological modulation".

REFERENCES

Cai, X.L., Zhu, J.S., Cao, J.M. & Cheng, X.Q., 2007. *3D structure and dynamic type of lithospheric crust in China mainland and adjacent areas*. Geology in China, 34 (4), 543-557, DOI:10.12029/gc20070401.

Cheng, B., Cheng, S.Y., Zhang, G.W. & Zhao, D.P., 2014. *Seismic structure of the Helan–Liupan–Ordos western margin tectonic belt in North-Central China and its geodynamic implications*. Journal of Asian Earth Sciences, 87 (12), 141-156, DOI:10.1016/j.jseaes.2014.01.006.

Deng, J., Wang, Q.F., Huang, D.H., Gao, B.F., Yang, L.Q. & Xu, T., 2005. *Evolution of basement and its control on cover layers in the Ordos Basin*. Earth Science Frontiers, (3), 91-99.

Ding, C., 2010. *Thermal evolution and petroleum-charging times in the Northeast area of Ordos Basin*. Thesis, Northwest University, Xi'an, China.

Gu, W., Weng, Y.W., Cao, G.Y. & Weng, S.L., 2007. *Research status and development trend of low-temperature thermal energy generation*. Thermal Power Engineering, 128(2), 115-119, 222.

Guo, M., Li, Z.D., Du, S.L. & Liu, S.P., 2009. *Origin of Upper Paleozoic formation water in Hangjinqi area and its relationship with oil and gas*. Minerals and Rocks, 29(1), 99-105, DOI:10.19719/j.cnki.1001-6872.2009.01.016.

Hu, S., He, L. & Wang, J.Y., 2001. *Compilation of geothermal flux data in the Chinese mainland (third edition)*. Chinese Journal of Geophysics, (5), 611-626, DOI:10.1002/cjg2.180.

Huang, F., He, L. & Wu, Q., 2015. *Characteristics of deep thermal structure in the Ordos Basin and its implications for the destruction of the North China Craton*. Chinese Journal of Geophysics, 58(10), 3671-3686, DOI:10.6038/cjg20151020.

Jiang, G.Z., Gao, P., Rao, S., Zhang, L.Y., Tang, X.Y., Huang, F., Zhao, P., Pang, Z.H., He, L.J., Hu, S.B. & Wang, J.Y., 2016. *Compilation of geothermal flux data in the Chinese mainland (fourth edition)*. Chinese Journal of Geophysics, 59(8), 2892-2910, DOI:10.6038/cjg20160815.

Li, B., 2021. *A Study of Tectonic-thermal Evolution History of Meso-Cenozoic Yimeng Uplift in the Ordos Basin*. Thesis, Northwest University, Xi'an, China.

Li, Q., Li, W.S., Zhang, X.J. & Zhuang, J.C., 1996. *Certain characteristics of geothermal distribution in Ergouduo and its surrounding areas*. Journal of Northwest Seismology, (2).

Lin, W., Liu, Z., Wang, W. & Wang G.-L., 2013. *The assessment of geothermal resources potential of China*. Geology in China, 40(1), 312-321, DOI:10.12029/gc20130121.

Qi, K., 2018. *A Preliminary Study of Meso-Cenozoic Thermal Regime and Lithospheric Dynamic Evolution in the Ordos Basin*. Thesis, Northwest University, Xi'an, China.

Qiao, J.X., 2013. *The Tectonic Evolution and Oil-gas Effect of Meso-Cenozoci Yimeng Uplift characteristics*. Thesis, Northwest University, Xi'an, China.

Quan, X.Y., 2020. *Paleozoic geological structure characteristics, its evolution and oil and gas occurrence in Yimeng uplift and its surrounding areas*. Thesis, Northwest University, Xi'an, China.

Ren, Z.L. & Zhao, C., 1997. *Comparative study on the thermal field of Mesozoic late period between the Ordos Basin and the Qinshui Basin*. Journal of Sedimentology, (2), DOI:10.14027/j.cnki.cjxb.1997.02.028.

Ren, Z.L., 1998. *Restoration and comparative study of the tectonic thermal evolution history of sedimentary basins in northern China.* Thesis, Northwest University, Xi'an, China.

Ren, Z.L, 2000. *Comparison of thermal evolution history of sedimentary basins in northern China*. Petroleum and Natural Gas Geology, (1), 33-37. DOI:10.11743/ogg20000108.

Ren, Z.L., Qi, K., Liu, R.C., Cui, J.P., Chen, Z.P., Zhang, Y.Y., Yang, G.L. & Ma, Q., 2020. *The dynamic background of the Early Cretaceous tectonic thermal events and their control on the formation of various mineral resources in the Ordos Basin and its periphery*. Journal of Rock Physics, 36(4), 1213-1234, DOI:10.18654/1000-0569/2020.04.15.

Ren, Z.L., Zhang, S., Gao, S.L., Cui, J.P. & Liu, X.S., 2006. *The relationship between thermal history and various energy minerals deposits in Dongsheng area, Yimeng Uplift*. Petroleum and Natural Gas Geology, (2), 187-193.

Ren, Z.L., Zhang, S., Gao, S.L., Cui J.P., Xiao Y.Y., &

Xiao H., 2007. *Tectonic thermal history and its significance on the formation of oil and gas accumulation and mineral deposit in Ordos Basin*., Science in China (Series D: Earth Sciences), (S1), 23-32, DOI:10.1007/s11430-007-6022-1.

Shao, Y., Ruan, Z., Yu, B. & Wu, Y., 2025. *Radiogenic heat production characteristics of rocks with varying ages and their dominant controlling factors, Dehong area, SW China*. Geothermics, 132:103436, DOI:10.1016/j.geothermics.2025.103436.

Sun, K., Fan, L.M., Ma, W.C., Chen, J.P., Peng, J., Zhang, P.H., Gao, S., Li, C., Miao, Y.P. & Wang, H.K., 2024. *Geochemical characteristics of groundwater in the Zhiluo Formation in the northern Ordos Basin and its implications*. Journal of Coal Science, 49(4), 2004-2020, DOI:10.13225/j.cnki.jccs.2023.0537

Sun, S., Liu, S. & Wang, J., 1996. *Characteristics of the geothermal field and the evolution of source rocks in the Ordos Basin*. Tectonics and Mineral Resources, (3).

Sun, Y.J., Dong, S.W., Fan, T.Y., Zhang H. & Shi, Y.L., 2013. *3D rheological structure of the continental lithosphere beneath China and adjacent regions*. Chinese Journal of Geophysics, 56(5), 546-558, DOI10.1002/cjg2.20052

Sun, Y., Zhao, C., Püttmann, W., Kalkreuth, W. & Qin, S., 2017. *Evidence of widespread wildfires in a coal seam from the Middle Permian of the North China Basin*. Lithosphere, 9; 4; 595–608, DOI:10.1130/L638.1.

Tang, B.N., Zhu, C.Q., Qiu, N.S., Cui, Y., Guo, S.S., Luo, X., Zhang, B.S., Li, K.Y., Li, W.Z. & Fu, X.D., 2021. *Analyzing and estimating thermal conductivity of sedimentary rocks from mineral composition and pore property*. Geofluids, 2021, 1-19, DOI:10.1155/2021/6665027.

Teng, J.W., Wang, F.Y., Zhao, W.Z. Zhang, Y-Q., Zhang, X-K., Yan, Y-F., Zhao, J-R., Li M., Yang, H., Zhang, H-S. & Ruan, X-M., 2010. *Velocity structure of layered block and deep dynamic process in the lithosphere beneath the Yinshan orogenic belt and Ordos Basin,* Chinese Journal of Geophysics, 53(1), 67-85, doi:10.3969/j.issn.0001-5733.2010.01.008

Tian, G., 2023. *Characteristics of basement faults in the northern part of the Ordos Block and their tectonic significance*. Thesis, China University of Petroleum (Beijing).

Wang, G., 2011. *Research on the source area and sequence stratigraphic lithofacies paleogeography of the Upper Paleozoic in the northern part of the Ordos Basin*. Thesis, Chengdu University of Technology.

Wang, G., Liu, Y., Zhu, X. & Zhang, W., 2020. *The status and development trend of geothermal resources in China*. Earth Science Frontiers, 27(1), 1-9.

Received: 29. 01. 2026
Revised: 03. 06. 2026
Accepted:24. 06. 2026
Published: 09. 07. 2026

Wang, G.L., Liu, Z.M. & Lin, W.J., 2004. *Tectonic Control of Geothermal Resources in the Peripheral of Ordos Basin*. Journal of Geology, (1), 44-51.

Wang, J. & Huang, S.P., 1988. *Compilation of geothermal flux data in the Chinese mainland*. Geological Sciences, (2), 196-204.

Wang, J. & Huang, S.P, 1990. *Compilation of geothermal flux data in the Chinese mainland (second edition)*. Seismology and Geology, (4), 351-363, 366.

Wang, G.L., Zhang, W., Liang, J.Y., Lin, W.J., Liu, Z.Y. & Wang, W.L., 2017. *Evaluation of Geothermal Resources Potential in China*. Acta Geoscientica Sinica, 38(4), 449-459, DOI:10.3975/cagsb.2017.04.02.

Wang, J.Y., Xiao, L., Li, P., Arbuzov, S.I. & Ding, S., 2019. *Occurrence mode of selected elements of coal in the Ordos Basin*. Energy Exploration & Exploitation, 37, 1680-1693, DOI:10.1177/0144598718763939.

Wang, M.J., Meng, X.J., Chen, X. & Zhu, X.Q., 2016. *Geochemistry and evaluation of upper paleozoic source rock on Yimeng Uplift, Ordos Basin*. Marine Geology Frontiers, 32(9), 26-31, DOI:10.16028/J.1009-2722.2016.09004.

Wei, Z.K., 2023. *Research on deep structure of the Ordos Basin based on gravity and magnetic data*. Thesis, Xi'an Petroleum University, Xi'an, China.

Yu, Q., Ren, Z.L., Li, R.X., Wang, B.J., Qin, X.L. & Tao, N., 2017. *Paleogeotemperature and maturity evolutionary history of the source rocks in the Ordos Basin*. Geological Journal, 52, 97-118, DOI:10.1002/gj.3069.

Zhang, L., 2017. *Gas emission and uranium mineralization effects in the northern part of the Ordos Basin*. Thesis, Northwest University, Xi'an, China.

Zhang, S., 2006. *The research on relationship between paleogeothermal evolutional history and various mineral deposits in ordos basin*. Thesis, Northwest University, Xi'an, China.

Zhang, Y.L., 1994. *Another contribution to the establishment of a new discipline of geological science of oil-bearing basins: Review of Zhao Chongyuan's new work "Research Progress of Oil-bearing Basins Geology"*. Journal of Northwest University (Natural Science Edition), (2).

Zhao, G.P., 2016. *Simulation study on the thermal evolution characteristics of Upper Paleozoic source rocks in Hangjinqi area of the Ordos Basin*. Petroleum Experimental Geology, 38(5), 641-646, DOI:10.11781/sysydz201605641.

Zhao, Y.Q., Ni, C.H., Wu, X.Q., Zhu, J.H., Liu, G.X., Wang, F.B., Jia, H.C., Zhang, W., Qi, R. & An, C., 2022. *Geochemical characteristics and source of Permian formation water in Hangjinqi area of the Ordos Basin*. Experimental Petroleum Geology, 44(2), 279-287, DOI:10.11781/sysydz202202279.7.